Observation of surface structure of 1-alkyl-3-methylimidazolium bis(trifluoromethanesulfonyl)imide using high-resolution Rutherford backscattering spectroscopy.

AUTHOR(S):

Nakajima, Kaoru; Ohno, Atsushi; Hashimoto, Hiroki; Suzuki, Motofumi; Kimura, Kenji

CITATION:

Nakajima, Kaoru ...[et al]. Observation of surface structure of 1-alkyl-3-methylimidazolium bis(trifluoromethanesulfonyl)imide using high-resolution Rutherford backscattering spectroscopy.. The Journal of chemical physics 2010, 133(4): 044702.

ISSUE DATE:

2010-07-28

URL:

http://hdl.handle.net/2433/128841

THE JOURNAL OF CHEMICAL PHYSICS **133**, 044702 (2010)

Observation of surface structure of 1-alkyl-3-methylimidazolium bis(trifluoromethanesulfonyl)imide using high-resolution Rutherford backscattering spectroscopy

Kaoru Nakajima, Atsushi Ohno, Hiroki Hashimoto, Motofumi Suzuki, and Kenji Kimura[a)]
Department of Micro Engineering, Kyoto University, Yoshida-honmachi, Sakyo, Kyoto 606-8501, Japan

(Received 28 April 2010; accepted 28 June 2010; published online 22 July 2010)

The surface structures of 1-alkyl-3-methylimidazolium bis(trifluoromethanesulfonyl)imide ([C_nMIM][TFSI], n=2,4,6) are studied by high-resolution Rutherford backscattering spectroscopy. The average composition of the surface molecular layer is very close to the stoichiometric composition, showing that neither ion is enriched in the surface layer. A detailed analysis indicates that both cations and anions have preferential molecular orientations at the surface. The alkyl chains of the [C_nMIM] cations protrude to the vacuum and the CF_3 groups of the [TFSI] anions are also pointing toward the vacuum. While the orientation of the [TFSI] anion becomes weaker with increasing alkyl-chain length, the protrusion of the alkyl chain occurs irrespective of the chain length. It was also found that the $N(SO_2)_2$ moiety is located nearly at the same depth as the imidazolium ring, suggesting that one of oxygen atoms in [TFSI] is bonded to the hydrogen of the C_2 carbon atom of the imidazolium ring. © *2010 American Institute of Physics*.
[doi:10.1063/1.3465578]

I. INTRODUCTION

Room-temperature ionic liquids (ILs) are thermally stable, nonvolatile, and nonflammable solvents. Because of these excellent properties, many promising applications, such as green chemical synthesis,[1–3] electrodeposition,[4–6] lithium ion batteries,[7,8] capacitors,[9,10] fuel cells, and[11,12] lubricants[13] have been extensively studied in the past decade. In these applications, understanding and control of surface properties is of great importance.

A pioneering study on the surface structure of IL (1-butyl-3-methylimidazolium hexafluorophosphate, [C_4MIM] [PF_6]) was performed by Gannon *et al.* using direct recoil spectroscopy (DRS). They found that there is no surface enrichment of either cations or anions.[14,15] By measuring incidence angle dependence of observed yield ratios of constitutent elements, it was shown that hydrogen is dominant in the outermost layer, carbon is located in the deeper region than hydrogen and fluorine is in the deepest region.[15] They also suggested that the butyl chain is almost parallel to the surface and the cation ring is perpendicular to the surface with the nitrogen atoms up.[15] After their measurements, various surface analysis techniques have been employed to study the surface structures of ILs.

Sum frequency generation (SFG) spectroscopy was used to study the surface structures of [C_nMIM] [BF_4] and [C_nMIM] [PF_6].[16–19] These studies suggested that the alkyl chains protrude to the vacuum, which is in contradiction to the DRS observation. Using x-ray reflectivity (XR) measurement, it was shown that there is a surface layer of 0.6–0.7 nm thickness, which has an electron density of 10%–12% higher than the bulk density in [C_4MIM] [PF_6] and [C_4MIM] [BF_4].[20] The origin of the observed electron-density enhancement was suggested to be the surface enrichment of the anion whose electron density is about three times larger than the cation. This observation, however, conflicts with the results of the SFG measurements.

In order to clear up the controversy about the surface structures of ILs, quantitative measurements of the surface composition should be useful. X-ray photoelectron spectroscopy (XPS) is one of the most popular techniques to measure the surface composition. Early studies using XPS showed that the surface composition of several ILs, including [C_nMIM] [PF_6], is stoichiometric,[21,22] suggesting neither surface enrichment of either ion nor preferential molecular orientation. However, XPS provides an average surface composition of a rather thick surface layer of a few nanometers. As a result, it is generally difficult to determine the structure of the topmost molecular layer from standard XPS measurements. Lockett *et al.*[23] demonstrated that qualitative composition of the outermost layer of ILs can be obtained using angle-resolved XPS (AR-XPS). They observed three imidazolium based ILs, [C_nMIM] [BF_4] (n=4,6,8) at various take-off angles (θ_e) ranging from 0° to 84°. They found that the signal of aliphatic carbon increases with increasing θ_e. This indicates that the alkyl chain is dominant at the surface in harmony with the SFG results but not with the XR result. Following their study, systematic AR-XPS measurements on various kinds of ILs have been performed.[24,25] As a result of these studies, a general consensus has been established that alkyl chains of [C_nMIM] cations protrude to the vacuum in [C_nMIM] [X] for $n \geq 4$ and the degree of the orientation increases with alkyl-chain length.

[a)]Author to whom correspondence should be addressed. Electronic mail: kimura@kues.kyoto-u.ac.jp.

In contrast to the [C_nMIM] cations, there are few studies about the behavior of anions. An AR-XPS study on [C_8MIM] [X] (X=nine different anions including bis(trifluoromethanesulfonyl)imide [TFSI]) showed that the anion is located nearly at the same depth as the imidazolium ring irrespective of the nature of the anion.[25] It was, however, difficult to observe a possible preferential orientation of the anion because the intensities of the anion-related photoelectron yields were very weak.[25] A signature of preferential orientation of anions was observed by low energy ion scattering spectroscopy (LEIS). There is only a fluorine signal in the LEIS spectrum of [C_4MIM] [TFSI], suggesting that the [TFSI] anions are oriented with their CF_3 groups pointing toward the vacuum.[22] Similar preferential orientation of the [TFSI] anion was also observed for [C_2MIM] [TFSI] using metastable impact electron spectroscopy (MIES) and ultraviolet photoelectron spectroscopy.[26] These techniques (LEIS and MIES) are, however, sensitive mainly to the outermost atomic layer and quantitative analysis is rather difficult. Recently, we employed high-resolution Rutherford backscattering spectroscopy (HRBS) to study the surface structure of trimethylpropylammonium bis(trifluoromethanesulfonyl)imide ([TMPA] [TFSI]).[27] HRBS provides quantitative depth profiling of ILs with a subnanometer depth resolution. We found that the surface is shared almost equally by the cations and anions. The C_1 conformer of [TFSI] anion is dominant among two stable conformers and the anions are oriented with their CF_3 groups pointing toward the vacuum in the outermost molecular layer. The anions in the second molecular layer also show a preferential orientation although it is rather weak.

So far, the preferential molecular orientation was observed for either the cation or the anion. In this paper, we observe [C_nMIM] [TFSI] (n=2,4,6) using HRBS. We found that both cations and anions have preferential orientations simultaneously. The alkyl chains protrude to the vacuum as was observed by AR-XPS and SFG. The [TFSI] anions also have preferential orientation with their CF_3 groups pointing toward the vacuum although the molecular orientation of [TFSI] becomes weaker with increasing alkyl-chain length of the [C_nMIM] cations.

II. EXPERIMENTAL

The details of the HRBS measurement were described elsewhere.[28] Briefly, He^+ ions are produced by a Penning ion gauge type ion source and accelerated up to 400 keV by a Cockcroft Walton type accelerator. The produced ion beam was mass analyzed by a deflecting magnet. The selected He^+ beam was collimated to 2×2 mm^2 by two sets of rectangular shaped slit system and sent to an ultrahigh-vacuum (UHV) scattering chamber via a differential pumping system. The typical beam current was about 50 nA and the base pressure of the UHV chamber was 1×10^{-8} Pa.

The [C_nMIM] [TFSI] (n=2,4,6) were purchased from Kanto Reagent (Japan) and measured by HRBS without further purification. In order to avoid possible radiation damage cause by the He^+ ion irradiation, we developed a target system which is a similar device developed by the previous pioneering works.[29,30] A slowly rotating wheel (diameter of 38 mm and rotation rate of 1.5–6 rpm) was partially immersed in a reservoir ($7\times40\times15$ mm^3) of IL so that the surface of the wheel was covered by a thin IL layer. The outermost part of the IL layer was removed by a skimmer (a razor blade) installed just above the reservoir to make a fresh and flat surface. Thus a thin fresh layer (~0.3 mm) of IL having a clean and flat surface was prepared. This wheel system was mounted on a precision goniometer in the UHV scattering chamber. After loading the IL, the UHV chamber was evacuated by a turbomolecular pump for more than 1 day. The HRBS spectra shown in this paper were measured after the chamber attained the vacuum in 10^{-7} Pa.

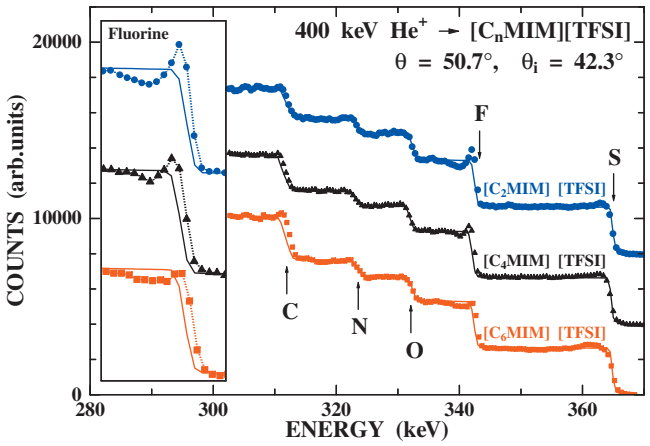

FIG. 1. HRBS spectra of [C_2MIM] [TFSI], [C_4MIM] [TFSI], and [C_6MIM] [TFSI] observed at a scattering angle θ=50.7°. The incident energy was 400 keV and the incident angle 42.3°. The solid lines show the calculated spectrum for uniform and stoichiometric composition. The agreement between the observed and calculated spectra is reasonably good except for a small structure seen in the observed spectra. The inset shows the magnified spectra around the fluorine edge.

The IL layer formed on the wheel surface was irradiated by the 400 keV He^+ beam. The He ions scattered from IL at a scattering angle θ=50.7° were energy analyzed by a 90° sector type magnetic spectrometer and detected by a one-dimensional position sensitive detector (1D-PSD) of 100 mm length (the energy window was 25% of the central energy). The nonuniformity of the efficiency of the 1D-PSD was carefully calibrated so that a precise composition analysis can be performed.

III. RESULTS AND DISCUSSION

Figure 1 shows examples of the HRBS spectra observed at an incident angle, θ_i=42.3° (exit angle was θ_e=87°) for [C_2MIM] [TFSI] (circles), [C_4MIM] [TFSI] (triangles), and [C_6MIM] [TFSI] (squares). There are several steps in the observed spectra. The energy of He ions scattered from a surface atom is given by KE_0, where E_0 is the incident energy of He^+ ion and K is a so-called kinematic factor,[31]

$$K=\left[\frac{(M_2^2-M_1^2\sin^2\theta)^{1/2}+M_1\cos\theta}{M_1+M_2}\right]^2, \quad (1)$$

where M_1 and M_2 are masses of the He ion and the target atom, respectively. When He ions are scattered from atoms inside the target, the energy of these ions is lower than KE_0 due to the energy loss during passage inside the target. Ac-

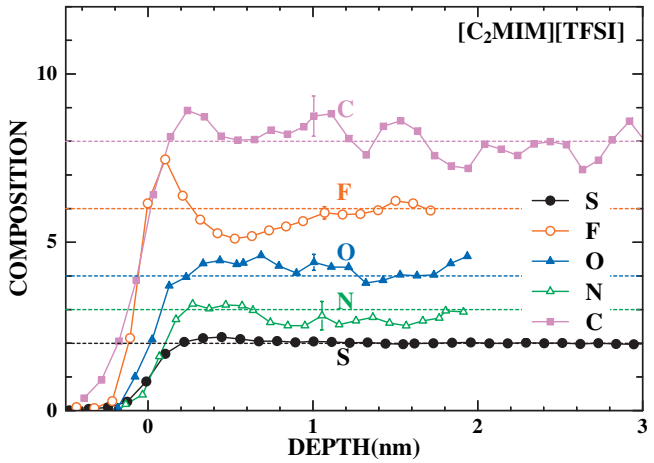

FIG. 2. Composition depth profiles for [C_2MIM] [TFSI] derived from the observed HRBS spectrum. Fluorine profile has a sharp peak at a depth of ~0.1 nm and a dip at a depth of ~0.5 nm. The depth resolution estimated from the shape of the leading edge of sulfur is better than 0.3 nm.

cordingly, steplike structures appear in the energy spectrum as is seen in Fig. 1. The step seen at the highest energy (~363 keV) corresponds to the heaviest element in the ILs, namely, sulfur. The energy scale shown in Fig. 1 was calibrated so that the energy of this step agrees with the calculated KE_0 for sulfur. The calculated KE_0 for F, O, N, and C are also shown by arrows in Fig. 1, which are in agreement with the observed steps. Please note that hydrogen cannot be measured under the present experimental conditions.

Figure 1 also shows simulated spectra for these ILs having stoichiometric composition by solid lines. The agreement between the measurement and the simulation is rather good, showing that the overall composition is close to the stoichiometric composition. Looking at the spectrum closely, a clear peak is seen at the leading edge of the fluorine signal in the observed spectra (see the inset). The fluorine peak is most pronounced for [C_2MIM] [TFSI] and becomes broader and smaller with increasing alkyl-chain length. There is also a small difference between the calculated and simulated spectra at the carbon edge. The observed carbon edge is shifted toward higher energies compared to the simulated spectrum. This energy shift becomes larger with increasing alkyl-chain length. Moreover, there is a small peak at the carbon leading edge for [C_6MIM] [TFSI].

These differences between the observed and simulated spectra indicate that the surface composition deviates from the stoichiomeric composition. Assuming that the deviation occurs only in the surface region, the observed HRBS spectrum can be decomposed into the contributions of the constituent elements with the help of the simulated spectrum. The details of the decomposition procedure were described in the previous paper.[27]

Figure 2 shows the decomposed spectra for [C_2MIM] [TFSI]. Here, the energy scale was converted into the depth scale using the following equation:[31]

$$E = K\left(E_0 - \frac{xS_{\text{in}}}{\cos\theta_{\text{i}}}\right) - \frac{xS_{\text{out}}}{\cos\theta_{\text{e}}}, \tag{2}$$

where x is the depth, and S_{in} and S_{out} are stopping powers in the incoming and outgoing trajectories of He ions, respectively. We used the stopping power of the bulk [C_2MIM] [TFSI] in this conversion. The scattering yield shown in the ordinate is normalized by the scattering cross section so that the spectra represent composition depth profiles. The typical errors are indicated by the bars. Lighter elements have larger errors because the scattering cross section is proportional to the square of the atomic number and the signals of lighter elements are always overlapped by those of heavier elements. Note that the depth scale shown here is just a relative scale. As was mentioned above, the energy scale was calibrated so that the sulfur leading edge appears at the calculated energy for a surface sulfur atom. Therefore the depth scale represents the depth with respect to the sulfur surface. It is also noteworthy that the depth profiles shown here are smeared by the depth resolution of HRBS and the depth resolution becomes worse with increasing depth due to energy loss straggling. We will discuss this effect later.

For comparison, the stoichiomeric composition is shown by dashed lines in Fig. 2. Although the observed profiles agree with the stoichiometric composition at a depth deeper than ~1 nm, the surface composition deviates from the stoichiometeric one. The fluorine profile has a sharp peak at ~0.1 nm. This sharp peak suggests surface enrichment of the anion because only the anion contains fluorine. In order to check if the anion is enriched at the surface, the average composition of the surface layer with 0.8 nm thickness (corresponding to one molecular layer) was calculated by integrating the composition profiles. The calculated composition, $S_{2.0}F_{6.2}O_{4.0}N_{2.5}C_{8.7}$, is close to the stoichiometric composition ($S_2F_6O_4N_3C_8$), showing that neither ion is enriched in the surface layer.

Similar fluorine surface peak was observed for [TMPA] [TFSI] and ascribed to the preferential molecular orientation of the [TFSI] anions at the surface, i.e., the [TFSI] anions are oriented with their CF_3 groups pointing toward the vacuum.[27] The [TFSI] anion has two stable conformers, C_1 and C_2. The C_2 conformer is energetically favorable and dominant in the bulk.[32] According to the discussion in our previous paper,[27] if the C_2 conformer is dominant at the surface, a second fluorine peak (contribution of the other CF_3 group in the same molecule) should appear at a depth about 0.5 nm deeper than the surface fluorine peak. There is no such second peak in the observed profile, indicating that the C_1 conformer is dominant at the surface of [C_2MIM] [TFSI], although the abundance of the C_2 conformer is estimated to be 80% at room temperature from the observed energy difference between two conformers [3.5 kJ mol^{-1} (Ref. 32)]. This discrepancy may be explained in terms of the extremely low surface energy of fluorine. When the CF_3 groups occupy the surface, the surface tension is considerably reduced. The reduction can be estimated from the surface tension difference between the ILs with and without the CF_3 group. For example, the surface tensions of [C_2MIM] [TFSI] and [C_2MIM] [$MeOSO_3$] (methyl sulfate) at room temperature are 35.7 and 62.9 mN m^{-1}, respectively.[33,34] Using the surface anion density of 1.8×10^{18} m^{-2} for [C_2MIM] [TFSI], this surface tension difference, 27.2 mN m^{-1}, corresponds to ~9 kJ mol^{-1}, which is large enough to compensate the energy difference between two conformers (3.5 kJ mol^{-1}).

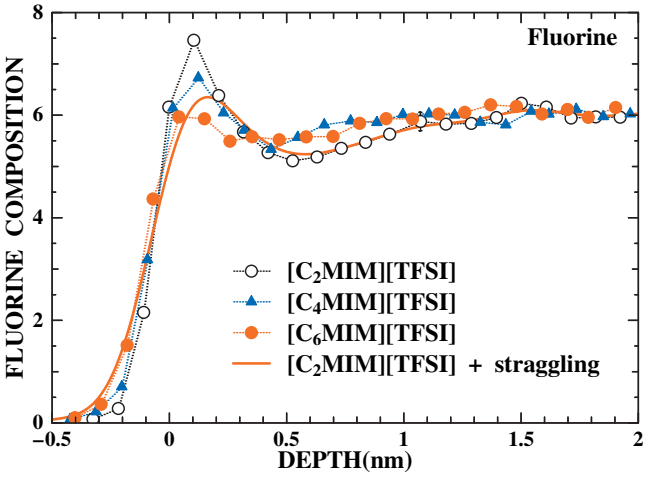

FIG. 3. Fluorine depth profiles for [C_2MIM] [TFSI] (open circles), [C_4MIM] [TFSI] (triangles), and [C_6MIM] [TFSI] (solid circles). The result of the convolution of the profile for [C_2MIM] [TFSI] with a Gaussian function representing the additional energy loss straggling is also shown by a solid line (see text). The peak seen in the observed profile for [C_6MIM] [TFSI] is weaker compared to the convoluted result, indicating that the orientation of [TFSI] in [C_6MIM] [TFSI] is weaker than that in [C_2MIM] [TFSI].

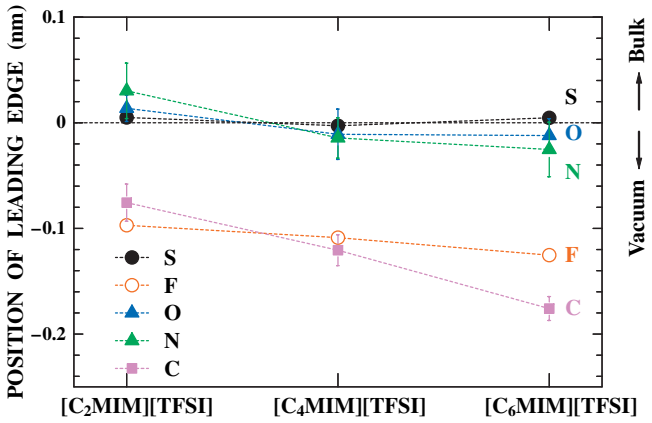

FIG. 4. The leading edge position of each element as a function of the alkyl-chain length of the cation. The positions of sulfur, oxygen, and nitrogen are almost the same, indicating that these elements are located nearly at the same depth. Fluorine and carbon are located outside of those three elements.

Now the origin of the preferential orientation of [TFSI] is clear, i.e., the surface occupation of CF_3 of [TFSI] reduces a substantial amount of the surface tension. This suggests surface segregation of [TFSI] anions, which however was not observed. This is because the Coulomb energy required for segregation of the anions is much larger than the surface tension reduction induced by the surface occupation of the CF_3 groups. When the first and the second molecular layers are occupied by the [TFSI] anions and the [C_nMIM] cations, respectively, the energy (per one ion pair) required to form such a dipole layer is given by

$$\frac{2e^2N_sd}{\varepsilon}, \tag{3}$$

where N_s is the surface density of ions, d is the width of the dipole layer, and ε is the dielectric constant of IL [typical value is ~10 (Ref. 35)]. Using Eq. (3), the Coulomb energy is estimated to be ~1.5 eV per ion pair (~14.5 kJ/mol), which is larger than the surface energy reduction induced by the surface occupation of the CF_3 groups of the [TFSI] anions. In our previous papers, we have observed surface structures of various ILs.[27,36,37] We found that all observed ILs are shared almost equally between cations and anions although preferential orientations of either cation or anion were observed in some cases. Similar structures were also observed using various other techniques.[14–19,21–26] This universal feature of ILs might be explained in the same manner.

The composition depth profiles for [C_4MIM] [TFSI] and [C_6MIM] [TFSI] were also derived from the observed HRBS spectra. The obtained profiles are basically the same as those of [C_2MIM] [TFSI] except for the fluorine profile. Figure 3 shows the comparison between the fluorine profiles for these ILs. All fluorine profiles have a surface peak, but the peak becomes weaker and broader with increasing alkyl-chain length. This suggests that the preferential molecular orientation of [TFSI] becomes weaker with increasing alkyl-chain length. The average compositions of the surface molecular layer of [C_4MIM] [TFSI] and [C_6MIM] [TFSI] were also calculated by integrating the profiles. The obtained average composition of the surface molecular layer are $S_{1.9}F_{6.2}O_{3.9}N_{2.5}C_{10.4}$ and $S_{1.8}F_{5.8}O_{3.5}N_{2.8}C_{13.5}$ for [C_4MIM] [TFSI] and [C_6MIM] [TFSI], respectively. These compositions are again very close to the stoichiometric ones, indicating that the surfaces of these ILs are also shared almost equally between cations and anions as is [C_2MIM] [TFSI].

Figure 4 shows the leading-edge positions of the elements in the composition depth profiles as a function of the alkyl-chain length. Note that the depth scale shown here is not the absolute one but the scale with respect to the sulfur surface as was mentioned above. The position shown in Fig. 4 is, therefore, a relative position with respect to the sulfur. The sulfur, oxygen, and nitrogen edges are located at the same position within the experimental error, indicating that these elements exist nearly at the same depth. This means that the $N(SO_2)_2$ moiety of [TFSI] exists nearby the imidazolium ring. It is generally believed that the C_2 hydrogen of the imidazolium ring plays an important role in cation-anion interactions (see Fig. 5).[38] The present result supports this picture, i.e., the hydrogen of the C_2 carbon atom is bonded to an oxygen atom of [TFSI].

The fluorine leading edge exists at a depth of about 0.1 nm outside these three elements (S, O, and N), irrespective of the alkyl-chain length. This is consistent with the above conclusion that the [TFSI] anion has a preferred orientation with CF_3 groups pointing toward the vacuum. The leading edge of carbon also exists outside those three elements (S, O,

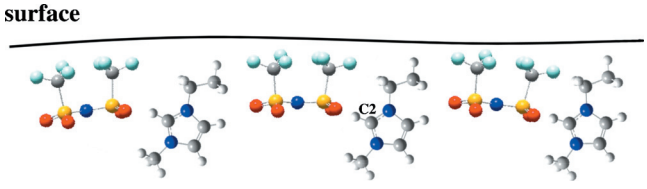

FIG. 5. Schematic drawing of the surface structures of [C_2MIM] [TFSI].

and N), indicating that the alkyl chains protrude to the vacuum as was observed by SFG (Refs. 16–19) and AR-XPS.[23–25] Such alkyl chains shield the polar part of the cation, i.e., the imidazolium ring, which reduces the electric field outside the surface and so reduces the surface energy. This could be the origin of the observed preferential orientation of [C_nMIM].

Considering all these findings, a surface structure model for [C_2MIM] [TFSI] can be derived, as shown in Fig. 5. The cations protrude their ethyl chains toward the vacuum. Regarding the [TFSI] anion, the C_1 conformer is dominant and their CF_3 groups are pointing toward the vacuum. The $N(SO_2)_2$ moieties of [TFSI] and the imidazolium rings are located nearly at the same depth and the hydrogen of the C_2 atom in the imidazolium ring is bonded to the oxygen atom in [TFSI]. This structure model is similar to that proposed by the AR-XPS studies.[24,25] The information of the molecular orientation of the [TFSI] anion, however, could not be obtained by AR-XPS because the intensities of the anion-related photoelectron yields were quite weak.[25] Moreover, for the cations having shorter alkyl chains ($n<4$), the protrusion of the alkyl chains was not clear in AR-XPS measurements. Here, using HRBS, the protrusion of the alkyl chain is clearly observed even for [C_2MIM].

In passing, we note that the observed carbon leading edge is shifted by ~0.05 nm when the number of carbon atoms in the alkyl chain increases by two (see Fig. 4). This is much smaller than the expected increase of the alkyl-chain length. This is because the depth scale shown here is derived using the stopping power of the bulk ILs. The stopping power of the alkyl-chain layer is much smaller than that of the bulk ILs. As a result, the shift is considerably underestimated. Taking account of the stopping power difference, the observed shift is consistent with the present structure model.

As can be seen from Fig. 3, the fluorine peak becomes broader with increasing alkyl-chain length. This suggests that the molecular orientation of the [TFSI] anion becomes weaker with increasing alkyl-chain length. Before concluding this, we have to check the influence of the energy loss straggling on the fluorine profile. Even if ions are scattered from the same atom, the energies of these ions are distributed around an average energy due to the stochastic nature of the energy loss process. This phenomenon is called energy loss straggling and the distribution is well approximated by a Gaussian distribution.[39] The energy loss straggling smears a real depth profile, $f_0(x)$, and the observed depth profile is given by

$$F(x) = f_0(x)^* G(\sigma,x), \tag{4}$$

where $G(\sigma,x)$ is a Gaussian distribution having a standard deviation σ, which represents the effect of the energy loss straggling, and * denotes convolution. Even if the molecular orientation of the [TFSI] anions in [C_6MIM] [TFSI] is the same as [C_2MIM] [TFSI], the observed fluorine profile $F_6(x)$ for [C_6MIM] [TFSI] is apparently different from the observed profile $F_2(x)$ for [C_2MIM] [TFSI] due to the additional energy loss straggling in the extra C_4H_8 layer. The resultant profile $F_6(x)$ is given by

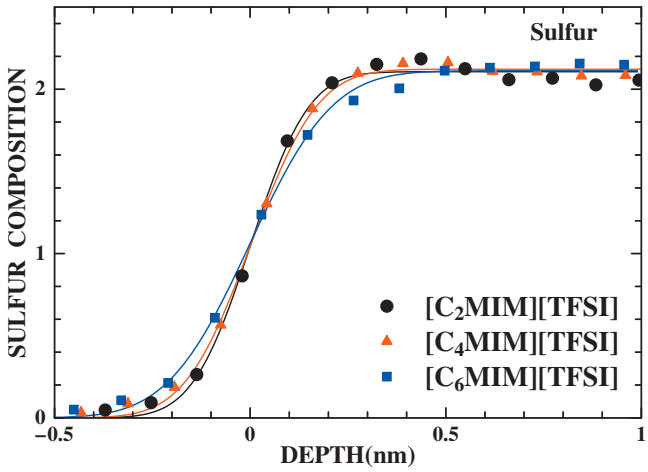

FIG. 6. Sulfur depth profiles for [C_2MIM] [TFSI], [C_4MIM] [TFSI], and [C_6MIM] [TFSI]. The profiles can be fitted to error functions, as shown by solid lines. The leading edge becomes broader with increasing alkyl-chain length, indicating that the preferential molecular orientation of the [TFSI] anion is disturbed stronger with increasing alkyl-chain length.

$$F_6(x) = f_0(x)^* G(\sigma,x)^* G(\Delta\sigma,x) = F_2(x)^* G(\Delta\sigma,x), \tag{5}$$

where $G(\Delta\sigma,x)$ represents the effect of the energy loss straggling in the extra C_4H_8 layer. Using a semiempirical formula for energy loss straggling,[40] $\Delta\sigma$ was estimated to be 0.07 nm. The fluorine profile $F_6(x)$ was calculated with Eq. (5) and the result (solid line) is compared with the observed profile (solid circles) in Fig. 3. Both profiles are similar but the surface peak in the observed profile is weaker compared to the calculated profile, indicating that the preferential orientation of [TFSI] in [C_6MIM] [TFSI] is somewhat disturbed as compared to [C_2MIM] [TFSI].

Another evidence of such a disturbance can be also seen in the sulfur profiles. Figure 6 shows the observed sulfur depth profiles for [C_2MIM] [TFSI], [C_4MIM] [TFSI], and [C_6MIM] [TFSI]. The distribution becomes broader with increasing alky-chain length. These sulfur profiles can be fitted to error functions reasonably well (solid lines). The standard deviation for these error functions are $\sigma_2=0.12$ nm and $\sigma_6=0.17$ nm for [C_2MIM] [TFSI] and [C_6MIM] [TFSI], respectively. If the orientation of [TFSI] does not change, σ_6 should be $(\sigma_2^2+\Delta\sigma^2)^{1/2}=0.14$ nm which is smaller than the observed $\sigma_6=0.17$ nm. This confirms that the preferential molecular orientation of the [TFSI] anion is disturbed in the [C_6MIM] [TFSI] as compared to [C_2MIM] [TFSI].

Detailed information of the [TFSI] at the surface of [C_6MIM] [TFSI] can be deduced from Fig. 3. The observed fluorine profile for [C_6MIM] [TFSI] (solid circles) has a peak at ~0.1 nm, which is weaker than the peak seen in the calculated profile (solid line). On the other hand, the observed fluorine concentration is larger than the calculated one around 0.6 nm, where a second fluorine peak is expected to appear for the C_2 conformer.[27] This suggests that a part of [TFSI] anions changes their structures from the C_1 conformer to the C_2 conformer as is schematically shown in Fig. 7. Although the C_1 conformer is energetically unfavorable, the surface energy can be lowered by exposing both CF_3 groups to the vacuum. This is the reason why the C_1 conformer is dominant at the surface of [C_2MIM] [TFSI]. For

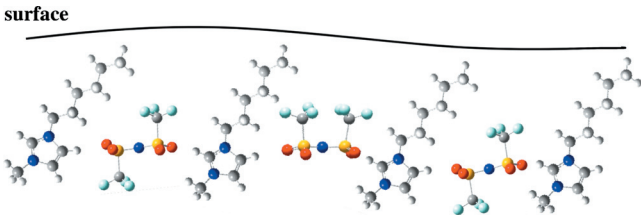

FIG. 7. Schematic drawing of the surface structure of [C_6MIM] [TFSI].

[C_6MIM] [TFSI], however, the situation is different. Because one of oxygen atoms in [TFSI] is bonded to the hydrogen of the C_2 carbon atom of the imidazolium ring, the CF_3 groups cannot be exposed to the vacuum (see Fig. 7).

It is known that ILs having longer alkyl chains have smaller surface tensions, e.g., the surface tensions of [C_2MIM] [$MeOSO_3$] and [C_4MIM] [$MeOSO_3$] are 62.9 and 44.1 mN m^{-1}, respectively.[33] The present result also indicates that longer alkyl chains have stronger tendency to occupy the surface, which disturbs the preferential orientation of the [TFSI] anions. This suggests that the surface of the mixture of [C_6MIM] [TFSI] and [C_2MIM] [TFSI] is enriched by [C_6MIM]. Figure 8 shows the composition depth profiles observed for the mixture of equal parts of [C_6MIM] [TFSI] and [C_2MIM] [TFSI]. For comparison, the average profiles of [C_6MIM] [TFSI] and [C_2MIM] [TFSI] are also shown by solid lines. The agreement between these profiles is very good, indicating that neither [C_6MIM] nor [C_2MIM] is enriched at the surface. This means that there is no notable difference between [C_6MIM] and [C_2MIM] in the tendency of occupying the surface in contradiction to the above expectation. This discrepancy can be explained in the following manner. If the surface is covered by [C_6MIM] [TFSI], the CF_3 groups of the [TFSI] cannot be exposed to the vacuum as was discussed in the preceding paragraph. As a result, the [TFSI] in [C_6MIM] [TFSI] cannot reduce the surface tension compared with the [TFSI] in [C_2MIM] [TFSI], that is to say, the overall surface tension of [C_6MIM] [TFSI] is not much smaller than that of [C_2MIM] [TFSI].

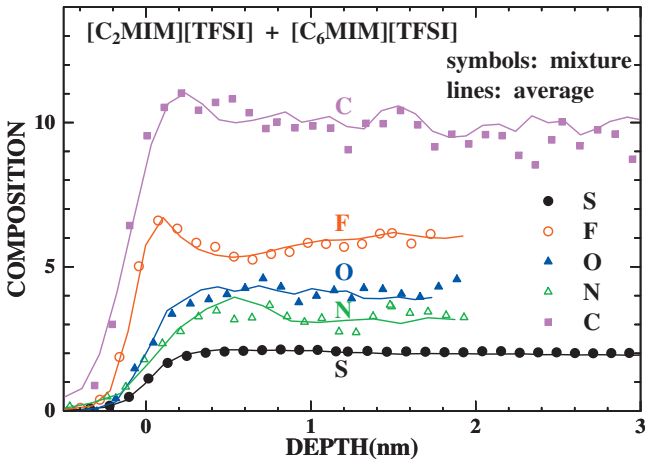

FIG. 8. Composition depth profiles observed for the mixture of equal parts of [C_6MIM] [TFSI] and [C_2MIM] [TFSI] (symbols). For comparison, the average profiles of [C_6MIM] [TFSI] and [C_2MIM] [TFSI] are also shown by solid lines. The agreement between these profiles is very good, indicating that neither [C_6MIM] nor [C_2MIM] is enriched at the surface.

IV. CONCLUSION

The surface structures of [C_2MIM] [TFSI], [C_4MIM] [TFSI], and [C_6MIM] [TFSI] were observed by HRBS. The surfaces are shared equally between cations and anions. Both cations and anions have preferential molecular orientations at the surface. The alkyl chains of the imidazolium cations protrude to the vacuum irrespective of the chain length. The C_1 conformer of the [TFSI] anion is dominant over the C_2 conformer and both CF_3 groups are pointing toward the vacuum at the surface of [C_2MIM] [TFSI]. This preferential orientation becomes weaker and fraction of C_2 conformer increases with increasing alkyl-chain length of the cation. We also found that the $N(SO_2)_2$ moiety of the [TFSI] anion is located nearly at the same depth as the imidazolium ring irrespective of the alkyl-chain length. The origin of these surface structures can be explained by the interaction between an oxygen atom of [TFSI] and the hydrogen of the C_2 carbon atom of the imidazolium ring and the preferential surface occupation of alkyl chains and CF_3 groups.

[1] P. Wasserscheid and W. Keim, Angew. Chem., Int. Ed. **39**, 3772 (2000).
[2] R. Sheldon, Chem. Commun. (Cambridge) **2001**, 2399.
[3] J. Dupont, R. F. Souza, and P. A. Suarez, Chem. Rev. (Washington, D.C.) **102**, 3667 (2002).
[4] P.-Y. Chen and I.-W. Sun, Electrochim. Acta **45**, 3163 (2000).
[5] F. Endres, ChemPhysChem **3**, 144 (2002).
[6] W. Freyland, C. A. Zell, S. Zein El Abedin, and F. Endres, Electrochim. Acta **48**, 3053 (2003).
[7] B. Garcia, S. Lavallée, G. Perron, C. Michot, and M. Armand, Electrochim. Acta **49**, 4583 (2004).
[8] H. Matsumoto, H. Sakaebe, and K. Tatsumi, J. Power Sources **146**, 45 (2005).
[9] M. Ue, M. Takeda, A. Toriumi, A. Kominato, R. Hagiwara, and Y. Ito, J. Electrochem. Soc. **150**, A499 (2003).
[10] Y. Kim, Y. Matsuzawa, S. Ozaki, K. C. Park, C. Kim, M. Endo, H. Yoshida, G. Masuda, T. Sato, and M. S. Dresselhaus, J. Electrochem. Soc. **152**, A710 (2005).
[11] A. Noda, A. Susan, K. Kudo, S. Mitsushima, K. Hayamizu, and M. Watanabe, J. Phys. Chem. B **107**, 4024 (2003).
[12] R. Hagiwara, T. Nohira, K. Matsumoto, and Y. Tamba, Electrochem. Solid-State Lett. **8**, A231 (2005).
[13] C. Ye, W. Liy, Y. Chen, and L. Yu, Chem. Commun. (Cambridge) **2001**, 2244.
[14] T. J. Gannon, G. Law, and P. R. Watson, Langmuir **15**, 8429 (1999).
[15] G. Law, P. R. Watson, A. J. Carmichael, and K. R. Seddon, Phys. Chem. Chem. Phys. **3**, 2879 (2001).
[16] S. Baldelli, J. Phys. Chem. B **107**, 6148 (2003).
[17] S. Rivera-Rubero and S. Baldelli, J. Am. Chem. Soc. **126**, 11788 (2004).
[18] T. Iimori, T. Iwahashi, H. Ishii, K. Seki, Y. Ouchi, R. Osawa, H. Hamaguchi, and D. Kim, Chem. Phys. Lett. **389**, 321 (2004).
[19] T. Iimori, T. Iwahashi, K. Kanai, K. Seki, J. Sung, D. Kim, H. Hamaguchi, and Y. Ouchi, J. Phys. Chem. B **111**, 4860 (2007).
[20] E. Sloutskin, B. M. Ocko, L. Tamam, I. Kuzmenko, T. Gog, and M. Deutsch, J. Am. Chem. Soc. **127**, 7796 (2005).
[21] E. F. Smith, F. J. M. Rutten, I. J. Villar-Garcia, D. Briggs, and P. Licence, Langmuir **22**, 9386 (2006).
[22] S. Caporali, U. Bardi, and A. Lavacchi, J. Electron Spectrosc. Relat. Phenom. **151**, 4 (2006).
[23] V. Lockett, R. Sedev, C. Bassel, and J. Ralston, Phys. Chem. Chem. Phys. **10**, 1330 (2008).
[24] K. R. J. Lovelock, C. Kolbeck, T. Cremer, N. Paape, P. S. Schulz, P. Wasserscheid, F. Maier, and H. P. Steinrück, J. Phys. Chem. B **113**, 2854 (2009).
[25] C. Kolbeck, T. Cremer, K. R. J. Lovelock, N. Paape, P. S. Schulz, P. Wasserscheid, F. Maier, and H.-P. Steinrück, J. Phys. Chem. B **113**, 8682 (2009).
[26] O. Höfft, S. Bahr, M. Himmerlich, S. Krischok, J. A. Schaefer, and V.

Kempter, Langmuir **22**, 7120 (2006).
[27] K. Nakajima, A. Ohno, M. Suzuki, and K. Kimura, Langmuir **24**, 4482 (2008).
[28] K. Kimura, S. Joumori, Y. Oota, K. Nakajima, and M. Suzuki, Nucl. Instrum. Methods Phys. Res. B **219–220**, 351 (2004).
[29] M. E. Saeckers, S. T. Govoni, D. V. Kowalski, M. E. King, and G. M. Nathanson, Science **252**, 1421 (1991).
[30] G. Andersson and H. Morgner, Surf. Sci. **405**, 138 (1998).
[31] For example, L. C. Feldman and J. W. Mayer, *Fundamentals of Surface and Thin Film Analysis* (North-Holland, Amsterdam, 1986), Chap. 5.
[32] K. Fujii, T. Fujimori, T. Takamuku, R. Kanzaki, Y. Umebayashi, and S. Ishiguro, J. Phys. Chem. B **110**, 8179 (2006).
[33] A. Wandschneider, J. K. Lehmann, and A. Heintz, J. Chem. Eng. Data **53**, 596 (2008).
[34] C. S. Santos and S. Baldelli, J. Phys. Chem. B **113**, 923 (2009).
[35] M. Mizoshiri, T. Nagano, Y. Mizoguchi, and M. Yao, J. Chem. Phys. **132**, 164510 (2010).
[36] A. Ohno, H. Hashimoto, K. Nakajima, M. Suzuki, and K. Kimura, J. Chem. Phys. **130**, 204705 (2009).
[37] H. Hashimoto, A. Ohno, K. Nakajima, M. Suzuki, H. Tsuji, and K. Kimura, Surf. Sci. **604**, 464 (2010).
[38] P. A. Hunt, J. Phys. Chem. B **111**, 4844 (2007).
[39] N. Bohr, K. Dan. Vidensk. Selsk. Mat. Fys. Medd. **18**, 8 (1948).
[40] Q. Yang, D. J. O'Connor, and Z. Wang, Nucl. Instrum. Methods Phys. Res. B **61**, 149 (1991).